Photo-reactivity of surfactants in the sea-surface microlayer and subsurface water of the Tyne estuary, UK

Philippa C. Rickard[1], Guenther Uher[1] and Robert C. Upstill-Goddard[1]

[1]School of Natural and Environmental Sciences, Newcastle University, Newcastle upon Tyne, UK.

Corresponding author: Philippa Rickard (philippa.rickard@ncl.ac.uk)

Key Points:

- Irradiation results in increased surfactant activity in the sea-surface microlayer and in subsurface water in the Tyne estuary (UK)
- Surfactant activity increased in parallel to photodegradation of chromophoric dissolved organic matter
- Insolation driven increases in sea-surface microlayer surfactant activity may have global implications for air-sea trace gas exchange

Abstract

We report the first estimates of total surfactant photo-reactivity in the sea-surface microlayer (SML) and in subsurface water (SSW) (Tyne estuary, UK; salinity 0.3-32.0). In addition to temperature, a known driver of surfactant adsorption kinetics, we show that irradiation contributes independently to enhanced interfacial surfactant activity (SA), a notion supported by coincident CDOM photodegradation. We estimate a mean SA production via irradiation of 0.064 $\pm$ 0.062 mg l^{-1} T-X-100 equivalents h^{-1} in the SML and 0.031 $\pm$ 0.025 mg l^{-1} T-X-100 equivalents h^{-1} in the SSW. Using these data, we derive first-order estimates of the potential suppression of the gas transfer velocity (k_w) by photo-derived surfactants ~12.9-48.9%. Given the ubiquitous distribution of natural surfactants in the oceans, we contend that surfactant photochemistry could be a hitherto unrecognized additional driver of air-sea gas exchange, with potential implications for global trace gas budgets and climate models.

Plain Language Summary

Surface-active substances (surfactants) are ubiquitous in seawater and freshwater. They accumulate in the uppermost < 1000 μm (surface microlayer) where they slow the rate of gas exchange between water and air. Improved knowledge of surfactant distributions and behaviour will improve global gas flux estimates (e.g. for CO_2) used to inform climate models. While increased temperature is known to enhance the microlayer accumulation of surfactants, further slowing gas exchange, our knowledge of other potentially important processes (e.g. surfactant photo-reactivity) is lacking. In the laboratory we simulated the natural solar irradiation of estuarine waters (Tyne, UK), and found surfactant enhancement additional to that from increased temperature, presumably reflecting photo-degradation of larger organic molecules. We argue that sunlight induced changes in other coastal waters, in the open ocean, and in freshwater will likely reflect differences in their organic compositions, prompting a need for wider investigation of this process.

1 Introduction

The sea surface microlayer (SML) impacts global element cycling and climate through the production, removal, and air-sea exchange of climate-active gases (Upstill-Goddard et al., 2003;

Cunliffe et al., 2013; Carpenter & Nightingale, 2015; Engel et al., 2017), and by generating marine boundary layer (MBL) aerosols (Facchini et al., 1999; Donaldson & George, 2012). Natural surfactants that are ubiquitous in seawater are enriched in the SML (Sabbaghzadeh et al., 2017; Wurl et al., 2011) via their adherence to the surfaces of rising bubbles that are generated during wave breaking (Robinson et al., 2019; Tseng et al., 1992), and which burst at the sea surface. This reduces the air-sea gas transfer velocity (k_w) of CO_2 and other gases by up to 50% (Frew, 2005; Salter et al., 2011; Pereira et. al., 2016; 2018), and following wind entrainment, impacts the MBL aerosol inventory (Leck & Bigg, 1999; Ovadnevaite et al., 2011; Kroflič et al., 2018).

High UV irradiance promotes high SML photo reactivity. Correlations of SML total surfactant activity (SA) with chromophoric dissolved organic matter (CDOM) absorbance (Sabbaghzadeh et al., 2017) are consistent with surfactant photo-reactivity, by analogy with CDOM photodegradation (Helms et al., 2008). Artificial surfactants produced volatile organics during irradiations of laboratory grade water (Fu et al., 2015; Alpert et al., 2017; Bernard et al., 2016), saline solutions (Ciuraru et al., 2015a, b), and artificial biofilms (Brüggemann et al., 2017). While photochemistry involving SML surfactants likely modifies k_w and MBL chemistry, photochemical changes to natural SML surfactants have yet to be unequivocally demonstrated. We therefore irradiated (solar simulator) contrasting salinity samples from the River Tyne estuary (UK), generating the first direct evidence for photochemical changes in SML SA. We compared these data with simultaneous changes in subsurface water (SSW) SA, and with corresponding changes in spectral CDOM characteristics, to evaluate the potential for air-sea gas exchange control by photochemically-derived surfactants in the SML.

2 Study Site and Sampling

The River Tyne (mean discharge 45 m^3 s^{-1}) enters the North Sea via the 35 km long Tyne estuary, which is macrotidal and partially mixed (Stubbins et al., 2010). We collected 13 estuarine samples (seven SML and six SSW: see supporting information) from four sites (TE1-TE4; Figure 1) spanning 0.3-32.0 salinity between the estuary mouth and 28 km upstream. SML sampling (June 2016 – January 2017) used a Garrett Screen (Garrett, 1965) (mesh: 16, wire diameter: 0.36 μm; effective surface area: 2025 cm^2) according to standard procedures (Gašparović et al., 2014) routine in our work (Pereira et al., 2016; Sabbaghzadeh et al., 2017).

Visual inspection prior to screen deployment precluded SML contamination by floating debris. TE1 was accessed using waders, avoiding entrainment of resuspended sediments. TE2-TE4 required a support vessel (RV *Princess Royal*) with the Garrett Screen hand-deployed over-side, minimizing potential contamination (engines off, wheelhouse and afterdeck downwind; Pereira et al., 2016). Sample volumes ~15 ml per dip equated to a 65-80 μm sampling depth. Twelve samples were unfiltered (supporting information) to retain SA associated with suspended particles (Ćosović & Vojvodić, 1987; Ćosović, 2005; Pereira et al., 2016; Schneider-Zapp et al., 2013). To discern photochemically mediated changes in SA and CDOM absorbance from those mediated by dissolved-particulate interactions and microbial processes, one sample (TE1; 30th January 2017; supporting information) was split into 0.22 μm filtered (Millex-GP polyethersulfone (PES) membrane) and unfiltered subsamples. For the irradiations we pooled SML samples from ~65 repeat deployments at each site (1000 cm^3). SSW sampling (~20 cm depth) used a clean 12-L steel bucket (*Princess Royal*) or 1-L polypropylene sample bottle (TE1). Sample storage bottles (1-L polypropylene) were aged (leachable organics-free), pre-washed (10% HCl acid; analytical grade water (milli-Q: ≥ 18.2 MΩ cm, Millipore System Inc., USA)), and filled to overflowing to preclude any headspace. Transport (< 3 hours) and storage pre-irradiation (< 48 hours) was at 4^{o}C in the dark (Schneider-Zapp et al., 2013).

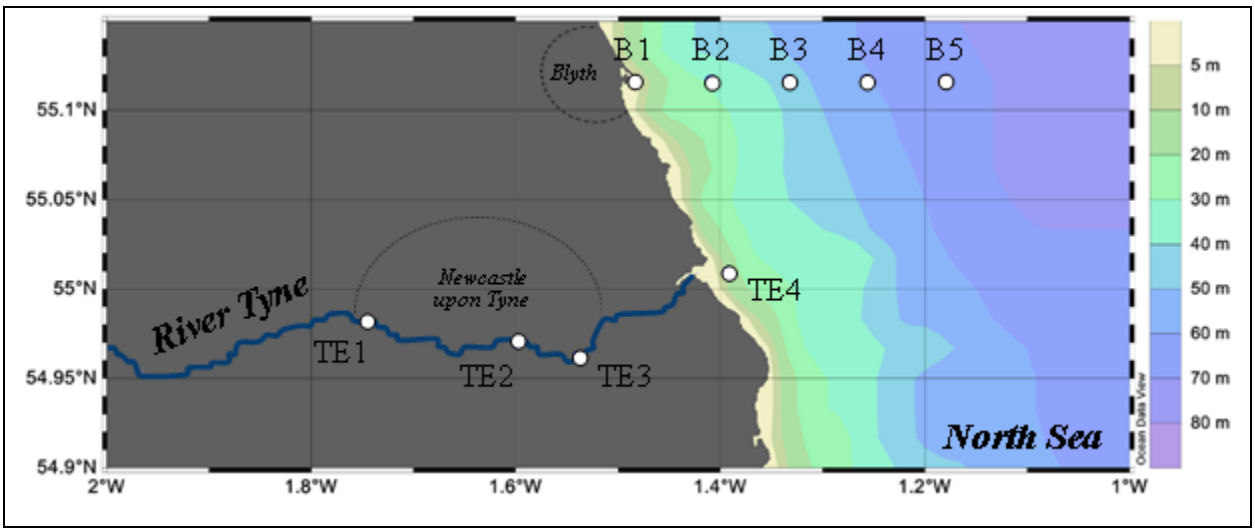

Figure 1 Tyne estuary (UK) sampling locations: TE4 (salinity 32.0) to TE1 (28 km upstream, salinity 0.3). Data from sites B1-B5 (Pereira et al., 2016) support our subsequent data interpretation. Colour bar indicates water depth (m). Map created with Ocean Data View: Schlitzer, R., https://odv.awi.de, (2018).

3 Irradiation Experiments

Irradiation experiments used a custom-designed solar simulator (Kitidis et al., 2008) and established procedures (e.g. Stubbins et al., 2011; Uher et al., 2017). The irradiation source (300 W Xenon-arc lamp: LOT Oriel; 300 nm transmission cut off) was borosilicate glass-sleeved to remove UVC radiation and surrounded by a motorized, 16 flask carousel. Total integrated spectral irradiance (247.8 W m^{-2}; 250-1050 nm; ILT950, LOT Quantum Design) exceeded mean July daily surface shortwave radiation (280-850 nm) for Newcastle upon Tyne (150-200 W m^{-2}; Hatzianastassiou et al., 2005) but was in the range of in situ daily maximum Global Horizontal Irradiance (GHI) during sampling (103.4-814.8 W m^{-2}; supporting information; copernicus.eu/; 240-4606 nm; Qu et al., 2017). Three experimental protocols used pre-combusted (450 °C; ≥4 h), 50 ml quartz irradiation flasks: (i) irradiated samples (IS: solar simulator, 14 experiments); (ii) dark controls (DC: double tin foil insulation, solar simulator, 14 experiments); (iii) temperature controls (TC: double tin foil insulation, 4 ℃ storage, 8 experiments). Sampling was at 0, 2, 4, 6, 8 and 24 hours, with 0-hour samples assumed to represent in situ conditions. Analytical constraints (irradiation duration, carousel spaces) precluded routine sample replication in individual experiments. We therefore replicated each experiment in full. Sample temperatures (unfiltered: IS, 19.1-28.5 ℃; DC, 17.0-24.6 ℃; TC, 7.6-17.3 ℃) were recorded immediately prior to SA analysis. CDOM sub-samples were immediately filtered (0.22 µm PES) and equilibrated to ambient temperature for 1 hour prior to analysis.

4 SA and CDOM analysis

All glassware was pre-combusted (450 °C; ≥4 h), acid washed (10% HCl) and rinsed (Milli-Q) between samples. SA was analyzed by hanging mercury drop, phase sensitive AC voltammetry (797VA Computrace, Metrohm, Switzerland) (Ćosović and Vojvodić, 1998). Calibration was against a nonionic soluble surfactant (Triton T-X-100 (Sigma-Aldrich, UK); mg L^{-1} T-X-100 equivalents) in a 0.55 mol L^{-1} NaCl matrix. Samples were adjusted to the ionic strength of the standards by adding NaCl solution (3 mol L^{-1}) to a maximum of 50 µL. Analytical precision was typically better than ±5%. We recorded CDOM absorbance (250-800 nm, 1 nm increments) on a UV-Visible double beam spectrophotometer (M550: Spectronic Camspec Ltd., UK), using 0.01 m pathlength cuvettes and a Milli-Q reference. We corrected for instrument drift, refractive

index effects and light scattering by residual particles by subtracting the mean 650-700 nm sample absorbance (Kitidis et al., 2006). Absorption spectra were derived from: $a = 2.303A/L$ (Kitidis et al., 2006), where A is the offset corrected wavelength-dependent absorbance (dimensionless) and L is optical pathlength (m). We adopted a_{300} (absorption coefficient at 300 nm) as a CDOM concentration proxy (Bricaud et al., 1981; Hu et al., 2002), as in previous studies of coastal and oceanic waters (Helms et al. 2013; Kitidis et al., 2006; Sabbaghzadeh et al., 2017).

5 Derived quantities and statistical analysis

We defined SA production during irradiation (mg L^{-1} T-X-100 eq. h^{-1}) as the difference between SA in irradiated samples (SA_{IS}) and dark controls (SA_{DC}) over time (T; 2 or 24 hours): $SA_{irr} = \frac{SA_{IS} - SA_{DC}}{T}$. The SA temperature effect was estimated as the difference between SA in dark controls (SA_{DC}) and temperature controls (SA_{TC}) over time (T; 2 or 24 hours): $SA_{temp} = \frac{SA_{DC} - SA_{TC}}{T}$. Following Helms et al. (2008), we derived CDOM spectral slopes (S; nm^{-1}) for the wavelength ranges 275-295 nm ($S_{275-295}$; nm^{-1}) and 350-400 nm ($S_{350-400}$; nm^{-1}), using: $a(\lambda) = a(\lambda_r)e^{-S(\lambda-\lambda_r)}$ (Helms et al., 2008), where a(λ) is the absorption coefficient (m^{-1}) at wavelength λ (nm) and λ_r is a reference wavelength (nm). These spectral slopes and the resulting spectral slope ratios ($S_R = S_{275-295}/S_{350-400}$) were used as broad indices of CDOM characteristics, including source, molecular weight, and degradation history (Helms et al., 2008; Kitidis et al., 2006).

All statistical procedures used SPSS. Data were screened for normality (Shapiro-Wilk tests), and correlations assessed using Kendall's-Tau correlation coefficient (null hypothesis: no significant SA vs CDOM correlation; significance 0.05) and the coefficient of determination ($R^2 \geq 0.5$ = strong correlation).

6 Results

CDOM behaviour over 24 hours irradiation followed established trends (e.g. Fichot & Benner, 2012; Helms et al., 2008), with a_{300} pseudo first-order half-lives ($t_{1/2}$) ~ 0.3-0.9 d. In IS, consistent increases in $S_{275-295}$ (6-29%) and S_R (12-35%) (supporting information) imply

irradiation induced decreases in CDOM molecular weight and aromaticity (Helms et al., 2008). Changes in $S_{350-400}$ were negligible over time and between experimental protocols (supporting information).

SA changes during irradiations indicated both photochemical and temperature effects in the SML and in SSW (Figure 2). For 64 of 67 time-points SA_{IS} exceeded SA_{DC}, for all time-points (39) SA_{IS} exceeded SA_{TC}, and for 38 of 39 time-points SA_{DC} exceeded SA_{TC}. The data thus confirm a photochemical SA source in the Tyne estuary. The largest changes in SA_{IS} consistently occurred during the initial 2 hours of irradiation and changes in both SA_{IS} and SA_{DC} were generally greater in the SML (SA_{IS}: 0.10-0.40 mg L^{-1} T-X-100 eq.; SA_{DC}: 0.03-0.40 mg L^{-1} T-X-100 eq.) than in SSW (SA_{IS}: 0.08-0.21 mg L^{-1} T-X-100 eq.; SA_{DC}: 0.03-0.14 mg L^{-1} T-X-100 eq.). In general, SA_{IS} increased over 24 hours in both SML and SSW (Figure 2, *a*,*b*,*e*,*f*,*h*,*j*-*n*), although some experiments showed overall decreases (Figure 2, *c* and *d*) or no discernable change (Figure 2, *g* and *i*). Comparison of initial SA in unfiltered and 0.22 μm filtered SML subsamples from TE1 (Figure 2, *g* and *h*) indicated a significant particle contribution (40%). Importantly, SA_{IS} increased in both subsamples during irradiation and remained higher than both SA_{DC} and SA_{TC}, consistent with photochemical SA production.

As our experimental design precluded SML interaction with SSW or air the variable changes in SA we observed (Figure 2) must reflect a dynamic balance between production and removal. To clarify the overall extent of SA change we subsequently consider only those production rates due to irradiation (SA_{irr}) and temperature (SA_{temp}) estimated over 0-2-hours (Table 1), the interval for which the greatest SA changes were consistently observed. These estimates are reasonable for our study area, for which total daylight ranged from ~7.5 hours (2 December 2016) to ~17.3 hours (27 June 2016) (supporting information). Although we also calculated SA_{irr} and SA_{temp} over 0-24-hours (Table 1), these do not represent conditions in situ.

Mean SA_{irr} (Table 1) was greater in the unfiltered SML than unfiltered SSW (0.064 ± 0.062 vs. 0.031 ± 0.027 mg L^{-1} T-X-100 eq. h^{-1} respectively), whereas mean SA_{temp} was greater in SSW than in the SML (0.056 ± 0.031 vs. 0.024 ± 0.054 mg L^{-1} T-X-100 eq. h^{-1} respectively). These values also show that in unfiltered SML samples, $SA_{irr} > SA_{temp}$, whereas in unfiltered SSW,

187 SA_{temp} > SA_{irr}. For the 0.22 μm filtered SML sample, the irradiation effect was slightly greater
188 than the temperature effect (0.030 vs 0.026 mg L^{-1} T-X-100 eq. h^{-1}).
189
190 A strong correlation between CDOM a_{300} and SA in initial (T_0) samples (τ (11) = 0.745, p =
191 0.001, R^2 = 0.874; supporting information), corroborates previous SA and CDOM data from
192 estuaries and the open ocean, where SA and CDOM negatively correlate with salinity (e.g.
193 Pereira et al., 2016, 2018; Uher et al., 2001). In many estuaries photochemical SA production
194 could be masked by strong lateral SA gradients from the mixing of high SA river water with low
195 SA coastal water (Pereira et al., 2016).
196
197 CDOM photodegradation (SML and SSW) coincided with SA photoproduction across the
198 salinity range sampled (0.3-32.0). CDOM is an important seawater surfactant component (e.g.
199 Tilstone, 2010) whose photodegradation in coastal and oceanic waters is widely documented
200 (Mopper et al., 2014). Ten of 12 irradiations where CDOM was quantified showed significant
201 positive correlations between SA and S_R ($p < 0.05$ for 10; $R^2 > 0.5$ for six), implying increased
202 SA during irradiation to be consistent with decreasing CDOM molecular weight. We therefore
203 contend that relatively low molecular weight surfactants are a likely by-product of CDOM
204 photodegradation in marine waters.
205
206 We found moderately strong positive correlations between SA_{irr} and initial $S_{350-400}$ (p = 0.015,
207 R^2 = 0.546, supporting information) but not for SA_{temp}, or for a_{300}, $S_{275-295}$ or S_R at T_0 ($p \geq$
208 0.176 and $R^2 \leq 0.098$; data not shown). This suggests that the initial chemical composition and
209 hence reactivity of the CDOM pool, rather than CDOM abundance, impacts rates of SA
210 production during irradiation.
211

212

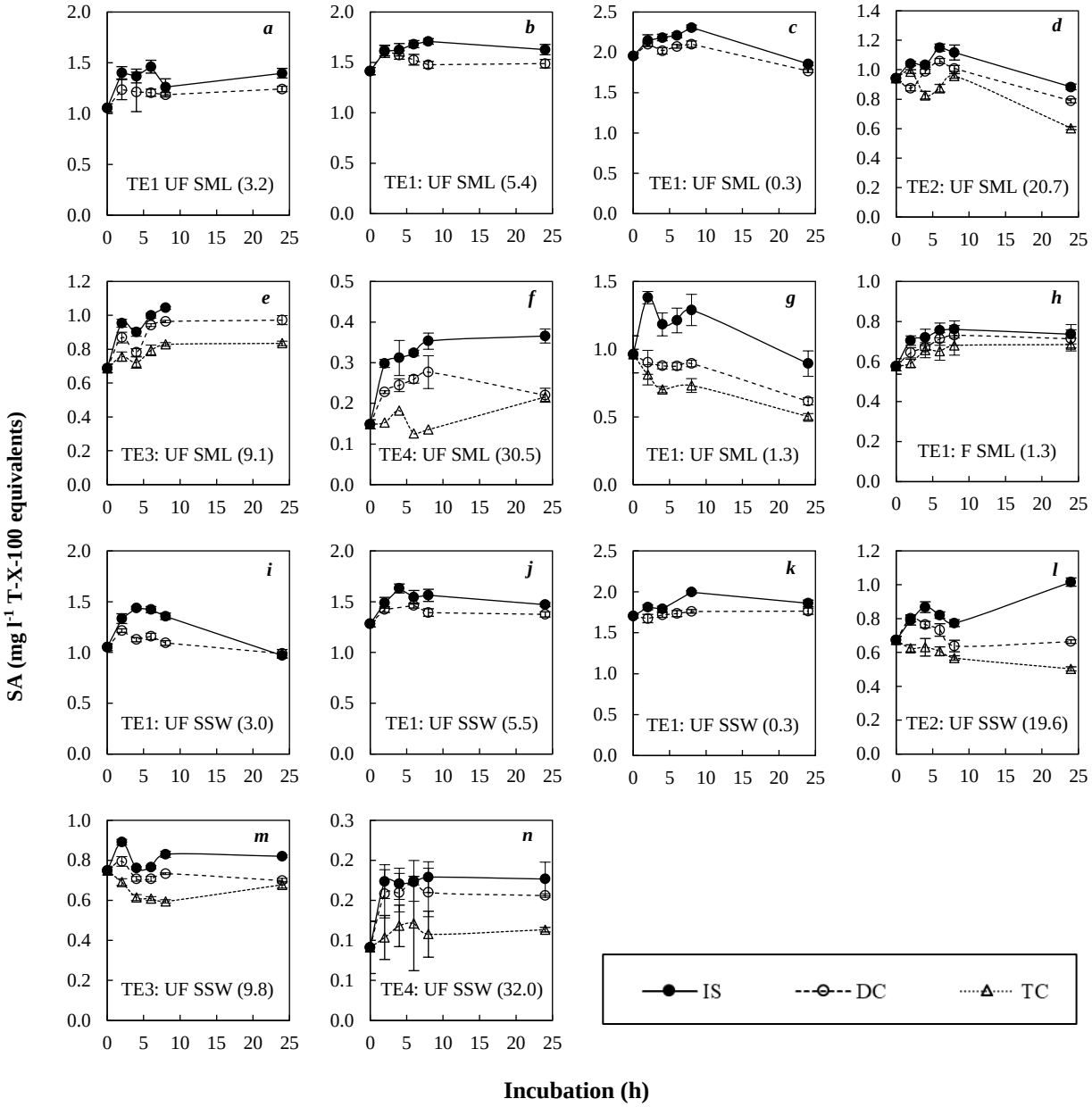

Figure 2 Changes in SA during 24-hour irradiations (sites TE1-TE4; Tyne estuary) for three experimental protocols: irradiated samples (IS), dark controls (DC) and temperature controls (TC). Sample designations are: UF (unfiltered); F (0.2 μm PES membrane filtered SML); SML (sea-surface microlayer); SSW (sub-surface water). The salinity of each sample is shown in brackets.

213

Table 1 SA production rates (mg l^{-1} T-X-100 eq. h^{-1}) estimated over 0-2 hours and 0-24 hours of irradiation for all Tyne estuary samples. SA production due to irradiation (SA_{irr}) is the difference in SA (mg l^{-1} T-X-100 eq.) between IS and DC at each timepoint (divided by the appropriate time) and SA production due to temperature (SA_{temp}) is the corresponding difference between DC and TC.

Sample description	Site	SA (mg l^{-1} T-X-100 equivalents h^{-1})			
		2 hours incubation		24 hours incubation	
		$\mathbf{SA_{irr}}$	$\mathbf{SA_{temp}}$	$\mathbf{SA_{irr}}$	$\mathbf{SA_{temp}}$
Unfiltered SML	TE1	0.083	-	0.006	-
(n = 7)	TE1	-0.004	-	0.006	-
	TE1	0.022	-	0.004	-
	TE2	0.083	-0.056	0.004	0.008
	TE3	0.042	0.056	-	0.006
	TE4	0.035	0.037	0.006	0.000
	TE1	0.186	0.057	0.010	0.005
	Mean ± σ	0.064 ± 0.062 *	-	0.006 ± 0.002 *	-
		0.087 ± 0.070 †	0.024 ± 0.054 †	0.007 ± 0.003 †	0.005 ± 0.003 †
0.22 μm filtered SML	TE1	0.030	0.026	0.001	0.001
(n = 1)					
Unfiltered SSW	TE1	0.036	-	0.024	-
(n = 6)	TE1	0.033	-	0.004	-
	TE1	0.069	-	0.004	-
	TE2	-0.006	0.089	0.015	0.007
	TE3	0.048	0.052	0.005	0.001
	TE4	0.008	0.027	0.001	0.002
	Mean ± σ	0.031 ± 0.025 *	-	0.008 ± 0.009 *	-
		0.017 ± 0.028 †	0.056 ± 0.031 †	0.007 ± 0.007 †	0.003 ± 0.003 †

* Mean and one standard deviation calculated using all available data.

† Mean and one standard deviation calculated using only experimental data where temperature controls were included as a sample treatment.

7 Discussion and Implications

We have shown the first evidence of coincident SA photoproduction and CDOM photodegradation in marine (estuarine) waters, although photoreactions implicating specific components of the marine surfactant pool are well established (e.g. Grzybowski, 2009; Kieber et al., 1997; Ortega-Retuerta et al., 2009). Our irradiations showed typical CDOM photobleaching

reflected in decreasing a_{300} and increasing S_R with time, indicative of decreases in dissolved organic matter (DOM) molecular weight.

Our irradiation data inevitably include a temperature related component due to warming that could cause increases in microbial production (e.g. Kurata et al., 2016) or the interfacial adsorption of surfactants due to entropic effects in the hydration shell (e.g. Gosálvez et al., 2009; Mohajeri & Dehghan Noudeh, 2012; Southall et al., 2001; Tielrooji et al., 2010), or an aggregate of both. At higher temperatures, the hydrogen bond network in the hydration shell is more dynamic (Tielrooji et al., 2010). Hence, an increase in temperature increases hydration shell entropy by breaking hydrogen bonds (Southall et al., 2001). Consequently, the size of the hydration shell diminishes, and surfactant adsorption density increases (Gosálvez et al., 2009). We contend that changes in surfactant adsorption behaviour are the likely dominant driver of temperature-related SA changes because the SA_{temp} data showed no concomitant changes in CDOM a_{300} or S_R. Microbial processing, adsorption and photodissolution cannot be excluded in these unfiltered water samples. Changes in CDOM spectral characteristics may be used to diagnose CDOM processing: increasing $S_{275-295}$ and S_R, and decreasing $S_{350-400}$ indicate photobleaching, while opposite trends indicate microbial alteration (Helms et al., 2008). However, $S_{350-400}$ changes during irradiations were negligible between sample treatments, suggesting that microbial activity followed the same trend in each.

A noteworthy feature was that irradiation *per se* was an independent driver of SA production, where SA_{irr} in the unfiltered SML (0.064 ± 0.062 mg L^{-1} T-X-100 equivalents h^{-1}) generally exceeded that in unfiltered SSW (0.031 ± 0.027 mg L^{-1} T-X-100 equivalents h^{-1}). Overall enrichments in relatively labile DOM compounds are an established feature of coastal systems (e.g. Galgani & Engel, 2016); these compounds transfer to the SML via bubble scavenging (Hardy, 1982; Robinson et al., 2019). Our data support the notion of SA photoproduction, either directly via the formation of new surface-active substances, or indirectly by photochemical transformations of existing surfactants allowing adsorption to the air-sea interface in greater numbers. CDOM photodegradation in parallel with SA photo-production strongly supports this concept.

250 Our data imply potential contributions of SML photochemistry to k_w suppression by surfactants
251 (e.g. Brockmann et al., 1982; Frew et al., 1990; Pereira et al., 2016; 2018; Ribas-Ribas et al.,
252 2018a; Salter et al., 2011) and to marine boundary layer aerosol and trace gas photochemistry
253 (Alpert et al., 2017; Bernard et al., 2016; Brüggemann et al., 2017; Ciuraru et al., 2015a; 2015b;
254 Clifford et al., 2008; Fu et al., 2015; Reeser et al., 2009; Rossignol et al., 2016) that demand
255 further scrutiny. Pereira et al (2018) applied a positive relationship between sea surface
256 temperature (SST) and k_w suppression at the ocean basin scale, implicating daily insolation as a
257 driver of surfactant production via primary productivity. Our results indicate that irradiation of
258 the SML is a likely important independent driver of SA production in addition to skin layer
259 temperature, and consequently is an important independent control on k_w.
260
261 It is instructive to estimate the potential scale of such control, by re-examining k_{660} (k_w for CO_2 in
262 seawater at 20 ℃) estimates for the coastal North Sea (B1-B5; Figure 1), made by Pereira et al.
263 (2016) in a gas exchange tank, that showed strong inverse relationships with SA. We applied
264 these to our T_0 irradiation data assuming them to represent in situ SA. This resulted in k_{660} values
265 of 0.6-13.4 cm h^{-1} spanning TE1-TE4 (salinity 0.3-32.0) consistent with values found by Pereira
266 et al (2016) and typical of other coastal sites (e.g. Kremer et al. 2003; Ribas-Ribas et al. 2018b).
267

Table 2. Projected k_{660} (cm h^{-1}) values, based on Pereira et al. (2016), for Tyne estuary SML and SSW SA at 0 hours and 2 hours irradiation (irradiated samples only), over a salinity gradient of 0.3 (TE1) to 32.0 (TE4).

Site	SML projected k_{660} (cm h^{-1}):			SSW projected k_{660} (cm h^{-1}):		
	0-hours	2-hours	Δ (%)	0-hours	2-hours	Δ (%)
TE1	0.59	1.48	44.1	0.90	2.24	18.9
TE1	1.45	1.05	28.1	1.81	1.28	29.2
TE1	2.65	0.43	27.3	2.76	0.75	16.7
TE1	3.66	1.87	48.9	-	-	-
TE1*	5.93	4.78	19.5	-	-	-
TE2	3.20	2.71	15.2	5.04	4.14	17.7
TE3	4.93	3.15	36.1	4.44	3.49	21.3
TE4	12.14	9.44	22.2	13.36	11.64	12.9

* 0.22 μm filtered SML sample.

268

Given that our most saline SML sample (TE4: salinity 30.5, SA 0.15 mg L^{-1} T-X-100 eq.; Figures 1 and 2*f*) was closest to the salinity range (33.1-34.6) given by Pereia et al. (2016) and within the respective SA range (0.08-0.38 mg L^{-1} T-X-100 eq.), we extended the Pereira et al. (2016) analysis to our 2-hour SA_{IS} data for TE4, which gives k_{660} suppressions of 22.2% (9.4 cm h^{-1} at 2-hours; SML) and 12.9% (11.6 cm h^{-1} at 2-hours; SSW) relative to T_0 k_{660} (12.1 and 13.4 cm h^{-1} respectively). Overall, unfiltered samples gave k_{660} suppressions of 15.2-48.9% (0.4-9.4 cm h^{-1} at 2-hours) in the SML and 12.9-29.3% (0.8-11.6 cm h^{-1} at 2-hours) in SSW, relative to respective T_0 k_{660}. Considering the range of k_{660} suppression by surfactants (Pereira et al. 2016), gas exchange control driven by photochemical changes could be considerable.

Due to the proximity of our samples to those of Pereira et al. (2016) (Figure 1), differences in organic composition between them, even when accounting for potential temporal variability, are likely to be smaller than contrasts with other geographical regions, and we note that SML surfactant photochemistry is yet to be explored in either oceanic waters or indeed in freshwater systems. Given that SML surfactant pool composition is likely to be important in addition to SA in controlling the magnitude of k_w (Pereira et al. 2016), regional to global differences in the composition of the SML surfactant pool and the attendant temporal variability will likely be reflected in a variable photochemical contribution to k_w control that demands further scrutiny.

5 Conclusions

Adequate parameterization of the factors controlling air-sea gas exchange is a long-standing scientific goal deemed essential to predicting global climate change. An increasing scientific focus is now on SML surfactant control of k_w (e.g. Brockmann et al., 1982; Frew et al., 1990; Pereira et al., 2016; 2018; Ribas-Ribas et al., 2018a; Salter et al., 2011). Temperature is a known control of surfactant adsorption kinetics, but we have shown irradiation to be an additional, independent driver, in parallel with CDOM photodegradation. We contend that photoinduced increases in SA will likely impede k_w at the global scale, with implications for the global budgets of climate-active gases. Consequently, studies of surfactant photo reactivity in a range of estuarine, coastal, and oceanic waters will be important, specifically those that examine how differences in total surfactant pool composition might differentially affect photochemistry and hence k_w.

Acknowledgments, Samples, and Data

This research was funded by the School of Marine Science and Technology, Newcastle University. We thank the crew of R/V *Princess Royal*, and David Murray, for field and logistical support, and Ryan Pereira and Bita Sabbaghzahdeh for technical advice. Supporting data are available at [currently included as supplement for review purposes; to be available in a community data repository in line with the FAIR Data Policy to provide access by acceptance].

References

Alpert, P.A., Ciuraru, R., Rossignol, S., Passananti, M., Tinel, L., Perrier, S., et al., 2017. Fatty Acid Surfactant Photochemistry Results in New Particle Formation. Scientific Reports, 7:12693. DOI:10.1038/s41598-017-12601-2

Bernard, F., Ciuraru, R., Boréave, A. & George, C., 2016. Photosensitized Formation of Secondary Organic Aerosols above the Air/Water Interface. Environmental Science & Technology, 50(16): 8678-8686.

Bricaud, A., Morel, A. & Prieur, L., 1981. Absorption by dissolved organic matter of the sea (yellow substance) in the UV and visible domains1. Limnology and Oceanography, 26(1): 43-53.

Brockmann, U.H., Hühnerfuss, H., Kattner, G., Broecker, H.C. & Hentzschel, G., 1982. Artificial surface films in the sea area near Sylt1. Limnology and Oceanography, 27(6): 1050-1058.

Brüggemann, M., Hayeck, N., Bonnineau, C., Pesce, S., Alpert. P.A., Perrier, S., et al., 2017. Interfacial photochemistry of biogenic surfactants: a major source of abiotic volatile organic compounds. Faraday Discussions, 200(0): 59-74.

Carpenter, L.J. & Nightingale, P.D., 2015. Chemistry and Release of Gases from the Surface Ocean. Chemical Reviews, 115(10): 4015-4034.

Ciuraru, R., Fine, L., van Pinxteren, M., D'Anna, B., Herrmann, H. & George, C., 2015a. Unravelling New Processes at Interfaces: Photochemical Isoprene Production at the Sea Surface. Environmental Science & Technology, 49(22): 13199-13205.

Ciuraru, R., Fine, L., van Pinxteren, M., D'Anna, B., Herrmann, H. & George, C., 2015b. Photosensitized production of functionalized and unsaturated organic compounds at the air-sea interface. Scientific Reports, 5: 12741.

Clifford, D., Donaldson, D.J., Brigante, M., D'Anna, B. & George, C., 2008. Reactive Uptake of Ozone by Chlorophyll at Aqueous Surfaces. Environmental Science & Technology, 42(4): 1138-1143.

Ćosović, B., 2005. Surface-Active Properties of the Sea Surface Microlayer and Consequences for Pollution in the Mediterranean Sea. 5K: 269-296.

Ćosović, B. & Vojvodić, V., 1982. The application of ac palarography to the determination of surface-active substances in seawater. Limnology and Oceanography, 27(2): 369-373.

Ćosović, B. & Vojvodić, V., 1987. Direct determination of surface active substances in natural waters. Marine Chemistry, 22: 363-373.

Ćosović, B. & Vojvodić, V., 1998. Voltammetric Analysis of Surface Active Substances in Natural Seawater. Electroanalysis, 10(6): 429-434.

Cunliffe, M., Engel, A., Frka, S., Gašparović, B., Guitart, C., Murrell, J.C., et al., 2013. Sea surface microlayers: A unified physicochemical and biological perspective of the air–ocean interface. Progress in Oceanography, 109:104-116. DOI:10.1016/j.pocean.2012.08.004

Donaldson, D.J. & George, C., 2012. Sea-Surface Chemistry and Its Impact on the Marine Boundary Layer. Environmental Science & Technology, 46(19): 10385-10389.

Engel, A. Bange, H.W., Cunliffe, M., Burrows, S.M., Friedrichs, G., Galgani, L., et al., 2017. The Ocean's Vital Skin: Toward an Integrated Understanding of the Sea Surface Microlayer. Frontiers in Marine Science, 4(165). DOI: 10.3389/fmars.2017.00165

Facchini, M.C., Mircea, M., Fuzzi, S. & Charlson, R.J., 1999. Cloud albedo enhancement by surface-active organic solutes in growing droplets. Nature, 401: 257.

Fichot, C.G. & Benner, R., 2012. The spectral slope coefficient of chromophoric dissolved organic matter (S275–295) as a tracer of terrigenous dissolved organic carbon in river-influenced ocean margins. Limnology and Oceanography, 57(5): 1453-1466.

Frew, N.M., 2005. The role of organic films in air-sea gas exchange, in The Sea Surface and Global Change, edited by P. S. Liss and R. A. Duce, pp. 121–171, Cambridge Univ. Press, U.K.

Frew, N.M., Goldman, J.C., Dennett, M.R. & Johnson, A.S., 1990. Impact of phytoplankton-generated surfactants on air-sea gas exchange. Journal of Geophysical Research, 95(C3): 3337.

Fu, H., Ciuraru, R., Dupart, Y., Passananti, M., Tinel, L., Rossignol, S., et al., 2015. Photosensitized Production of Atmospherically Reactive Organic Compounds at the Air/Aqueous Interface. Journal of the American Chemical Society, 137(26): 8348-8351.

Galgani, L. & Engel, A., 2016. Changes in optical characteristics of surface microlayers hint to photochemically and microbially mediated DOM turnover in the upwelling region off the coast of Peru. Biogeosciences, 13(8): 2453-2473.

Garrett, W.D., 1965. Collection of slick-forming materials from the sea surface. 602-605.

Gašparović, B., Laß, K., Frka, S., Reunamo, A., Yang, G-P., & Upstill–Goddard, R., 2014. Sampling technique: Screen samples. In: Cunliffe, M. & Wurl, O. (Editors), Guide to best practices to study the ocean's surface.

Gosálvez, M.A., Tang, B., Pal, P., Sato, K., Kimura, Y. & Ishibashi, K., 2009. Orientation- and concentration-dependent surfactant adsorption on silicon in aqueous alkaline solutions: Explaining the changes in the etch rate, roughness and undercutting for MEMS applications. Journal of Micromechanics and Microengineering, 19(12).

Grzybowski, W., 2009. Terrestrial humic substances induce photodegradation of polysaccharides in the aquatic environment. Photochem Photobiol Sci, 8(10): 1361-3.

Hardy, J.T., 1982. The Sea Surface Microlayer: Biology, Chemistry and Anthropogenic Enrichment. Progress in Oceanography, 11: 307-328.

Hatzianastassiou, N., Matsoukas, C., Fotiadi, A., Pavlakis, K.G., Drakakis, E., Hatzidimitriou, D., et al., 2005. Global distribution of Earth's surface shortwave radiation budget, Atmospheric Chemistry and Physics, 5, 2847–2867. DOI:10.5194/acp-5-2847-2005.

Helms, J.R., Stubbins, A., Ritchie, J.D., Minor, E.C., Kieber, D.J. & Mopper, K., 2008. Absorption Spectral Slopes and Slope Ratios as Indicators of Molecular Weight, Source, and Photobleaching of Chromophoric Dissolved Organic Matter. Limnology and Oceanography, 53(3): 955-969.

Helms, J.R., Stubbins, A., Perdue, E.M., Green, N.W., Chen, H. & Mopper, K., 2013. Photochemical bleaching of oceanic dissolved organic matter and its effect on absorption spectral slope and fluorescence. Marine Chemistry, 155: 81-91.

Hu, C., Muller-Karger, F.E. & Zepp, R.G., 2002. Absorbance, absorption coefficient, and apparent quantum yield: A comment on common ambiguity in the use of these optical concepts. Limnology and Oceanography, 47(4): 1261-1267.

Kieber, R.J., Hydro, L.H. & Seaton, P., 1997. Photooxidation of triglycerides and fatty acids in seawater: Implication toward the formation of marine humic substances. Limnology and Oceanography, 42(6): 1454-1462.

Kitidis, V., Stubbins, A.P., Uher, G., Upstill-Goddard, R.C., Law, C.S. & Woodward, E.M.S., 2006. Variability of chromophoric organic matter in surface waters of the Atlantic Ocean. Deep Sea Research Part II: Topical Studies in Oceanography, 53(14): 1666-1684.

Kitidis, V., Uher, G., Woodward, E.M.S., Owens, N.J.P. & Upstill-Goddard, R.C., 2008. Photochemical production and consumption of ammonium in a temperate river–sea system. Marine Chemistry, 112(1-2): 118-127.

Kremer, J.N., Reischauer, A. & D'Avanzo, C., 2003. Estuary-Specific Variation in the Air-Water Gas Exchange Coefficient for Oxygen. Estuaries, 26(4): 829-836.

Kroflič, A., Frka, S., Simmel, M., Wex, H. & Grgić, I., 2018. Size-Resolved Surface-Active Substances of Atmospheric Aerosol: Reconsideration of the Impact on Cloud Droplet Formation. Environmental Science & Technology, 52(16): 9179-9187.

Kurata, N., Vella, K., Hamilton, B., Shivji, M., Soloviev, A., Matt, S., et al., 2016. Surfactant-associated bacteria in the near-surface layer of the ocean, Nature Scientific Reports, 19123, DOI:10.1038/srep19123.

Leck, C. & Bigg, E.K., 1999. Aerosol production over remote marine areas—A new route, Geophysical Research Letters, 26, 3577–3580, doi:10.1029/1999GL010807.

Mohajeri, E. & Dehghan Noudeh, G., 2012. Effect of Temperature on the Critical Micelle Concentration and Micellization Thermodynamic of Nonionic Surfactants: Polyoxyethylene Sorbitan Fatty Acid Esters, Journal of Chemistry, 9(4), 2268-2274. DOI:10.1155/2012/961739

Mopper, K., Kieber, D.J. & Stubbins, A., 2014. Marine Photochemistry of Organic Matter: Processes and Impacts. In: D.A. Hansell and C.A. Carlson (Editors), Biogeochemistry of marine dissolved organic matter. Amsterdam: Academic Press.

Ovadnevaite, J., O'Dowd, C., Dall'Osto, M., Ceburnis, D., Worsnop, D.R. & Berresheim, H., 2011. Detecting high contributions of primary organic matter to marine aerosol: A case study, Geophys. Res. Lett., 38, L02807, doi:10.1029/2010GL046083

Ortega-Retuerta, E., Passow, U., Duarte, C.M. & Reche, I., 2009. Effects of ultraviolet B radiation on (not so) transparent exopolymer particles. Biogeosciences Discuss, 6: 7599-7625.

Pereira, R., Ashton, I., Sabbaghzadeh, B., Shutler, J.D. & Upstill-Goddard, R.C., 2018. Reduced air–sea CO_2 exchange in the Atlantic Ocean due to biological surfactants. Nature Geoscience, 11(7): 492-496.

Pereira, R., Schneider-Zapp, K. & Upstill-Goddard, R., 2016. Surfactant control of gas transfer velocity along an offshore coastal transect: results from a laboratory gas exchange tank, 1-17 pp.

Qu, Z., Oumbe, A., Blanc, P., Espinar, B., Gesell, G., Gschwind, B., et al., 2016. Fast radiative transfer parameterisation for assessing the surface solar irradiance: The Heliosat-4 method. Contributions to Atmospheric Sciences, 26(1): 33-57.

Ribas-Ribas, M., Helleis, F., Rahlff, J. & Wurl, O., 2018a. Air-Sea CO_2-Exchange in a Large Annular Wind-Wave Tank and the Effects of Surfactants. Frontiers in Marine Science, 5(457).

Ribas-Ribas, M., Kilcher, L.& Wurl, O., 2018b. Sniffle: A step forward to measure in situ CO_2 fluxes with the floating chamber technique, 6, 14 pp.

Reeser, D.I., Jammoul, A., Clifford, D., Brigante, M., D'Anna, B., George, C., et al., 2009. Photoenhanced Reaction of Ozone with Chlorophyll at the Seawater Surface. The Journal of Physical Chemistry C, 113(6): 2071-2077.

Robinson, T.-B., Wurl, O., Bahlmann, E., Jürgens, K. & Stolle, C., 2019. Rising bubbles enhance the gelatinous nature of the air–sea interface. Limnology and Oceanography, 64: 2358-2372. DOI:10.1002/lno.11188

Rossignol, S. Tinel, L., Bianco, A., Passananti, M., Brigante, M., Donaldson, D.J., et al., 2016. Atmospheric photochemistry at a fatty acid–coated air-water interface. Science, 353(6300): 699-702.

Sabbaghzadeh, B., Upstill-Goddard, R.C., Beale, R., Pereira, R. & Nightingale, P.D., 2017. The Atlantic Ocean surface microlayer from 50°N to 50°S is ubiquitously enriched in surfactants at wind speeds up to 13 m s^{-1}. Geophysical Research Letters, 44(6): 2852-2858.

Salter, M.E., Upstill-Goddard, R.C., Nightingale, P.D., Archer, S.D., Blomquist, B., Ho, D.T., et al., 2011. Impact of an artificial surfactant release on air-sea gas fluxes during Deep Ocean Gas Exchange Experiment II. Journal of Geophysical Research, 116(C11).

Schneider-Zapp, K., Salter, M.E., Mann, P.J. & Upstill-Goddard, R.C., 2013. Technical Note: Comparison of storage strategies of sea surface microlayer samples. Biogeosciences, 10(7): 4927-4936.

Southall, N.T., Dill, K.A. & Haymet, A.D.J., 2002. A View of the Hydrophobic Effect, Journal of Physical Chemistry B, 106, 3, 521–533

Stubbins, A., Law, C.S., Uher, G. & Upstill-Goddard, R.C., 2011. Carbon monoxide apparent quantum yields and photoproduction in the Tyne estuary. Biogeosciences, 8(3): 703-713.

Stubbins, A., Uher, G., Kitidis, V., Law, C.S., Upstill-Goddard, R.C. & Woodward, E.M.S., 2006. The open-ocean source of atmospheric carbon monoxide. Deep Sea Research Part II: Topical Studies in Oceanography, 53(14-16): 1685-1694.

Tielrooij, K-J., Hunger, J., Buchner, R., Bonn, M. & Bakker, H.J., 2010. Influence of Concentration and Temperature on the Dynamics of Water in the Hydrophobic Hydration Shell of Tetramethylurea, Journal of the American Chemical Society, 132, 44, 15671–15678.

Tilstone, G.H., Airs, R.L., Vicente, V.M., Widdicombe, C. & Llewellyn, C., 2010. High concentrations of mycosporine-like amino acids and colored dissolved organic matter in the sea surface microlayer off the Iberian Peninsula. Limnology and Oceanography, 55(5): 1835-1850.

Tseng, R.-S., Viechnicki, J.T., Skop, R.A., & Brown, J.W., 1992. Sea-to-air transfer of surface-active organic compounds by bursting bubbles, Journal of Geophysical Research, 97(C4), 5201– 5206, doi:10.1029/91JC00954.

Uher, G., Hughes, C., Henry, G. & Upstill-Goddard, R.C., 2001. Non-conservative mixing behavior of colored dissolved organic matter in a humic-rich, turbid estuary. Geophysical Research Letters, 28(17): 3309-3312.

Uher, G., Pillans, J.J., Hatton, A.D. & Upstill-Goddard, R.C., 2017. Photochemical oxidation of dimethylsulphide to dimethylsulphoxide in estuarine and coastal waters. Chemosphere, 186: 805-816.

Upstill-Goddard, R.C., Frost, T., Henry, G.R., Franklin, M., Murrell, J.C. & Owens, N.J.P., 2003. Bacterioneuston control of air-water methane exchange determined with a laboratory gas exchange tank. Global Biogeochemical Cycles, 17(4): 1108.

Wurl, O., Wurl, E., Miller, L., Johnson, K. & Vagle, S., 2011. Formation and global distribution of sea-surface microlayers. Biogeosciences, 8(1): 121-135.